Enhanced expression of MycN/CIP2A drives neural crest toward a neural stem cell-like fate: Implications for priming of neuroblastoma

Laura Kerosuo[a], Pushpa Neppala[a,b], Jenny Hsin[a], Sofie Mohlin[c], Felipe Monteleone Vieceli[a], Zsofia Török[a], Anni Laine[b], Jukka Westermarck[b,d], and Marianne E. Bronner[a,1]

[a]Department of Biology and Biological Engineering, California Institute of Technology, Pasadena, CA 91125; [b]Turku Centre for Biotechnology, University of Turku and Åbo Akademi University, FI-20014 Turku, Finland; [c]Pediatric Oncology, Department of Clinical Sciences Lund, Lund University, SE-22381 Lund, Sweden; and [d]Institute of Biomedicine, University of Turku, FI-20014 Turku, Finland

Contributed by Marianne E. Bronner, June 13, 2018 (sent for review January 3, 2018; reviewed by Angela Nieto and Carol Thiele-Galetto)

Neuroblastoma is a neural crest-derived childhood tumor of the peripheral nervous system in which MycN amplification is a hallmark of poor prognosis. Here we show that *MycN* is expressed together with phosphorylation-stabilizing factor *CIP2A* in regions of the neural plate destined to form the CNS, but MycN is excluded from the neighboring neural crest stem cell domain. Interestingly, ectopic expression of MycN or CIP2A in the neural crest domain biases cells toward CNS-like neural stem cells that express Sox2. Consistent with this, some forms of neuroblastoma have been shown to share transcriptional resemblance with CNS neural stem cells. As high *MycN/CIP2A* levels correlate with poor prognosis, we posit that a MycN/CIP2A-mediated cell-fate bias may reflect a possible mechanism underlying early priming of some aggressive forms of neuroblastoma. In contrast to *MycN*, its paralogue *cMyc* is normally expressed in the neural crest stem cell domain and typically is associated with better overall survival in clinical neuroblastoma, perhaps reflecting a more "normal" neural crest-like state. These data suggest that priming for some forms of aggressive neuroblastoma may occur before neural crest emigration from the CNS and well before sympathoadrenal specification.

neuroblastoma initiation | MycN | CIP2A | neural crest | Sox2

Neuroblastoma is the most common extracranial solid tumor in childhood. Typically occurring before the age of 2 y with a prevalence of 2.5–5 cases per 100,000 people (1), neuroblastoma is thought to be a neural crest-derived tumor of sympathetic ganglia, most commonly located in the adrenal glands. Amplification of the transcription factor *MycN* occurs in ∼20% of all neuroblastoma cases and is associated with aggressive disease with a poor prognosis (2–4). Given the early onset of neuroblastoma, it has been speculated that tumor initiation may reflect abnormal deployment of events occurring at early stages of nervous system development. In recent years, research in the field has focused on tumorigenic changes in sympathoadrenal precursors. In contrast, little attention has been given to the possible involvement of earlier events in neural crest development in neuroblastoma onset.

The neural crest is a transient population of multipotent stem cells that is induced during gastrulation at the neural plate border, a region between the neural plate (the future CNS) and the nonneural ectoderm (the future epidermis). After neural tube closure, premigratory neural crest cells are initially contained with the dorsal midline of the forming CNS. Subsequently, neural crest cells undergo an epithelial-to-mesenchymal transition (EMT) to delaminate from the dorsal neural tube and initiate migration toward various destinations within the body. Upon localization at their final sites, they differentiate into a myriad of different cell types, including the neurons and glia of the peripheral nervous system (PNS), melanocytes, and endocrine cells, as well as facial bone and cartilage (5).

The Myc family of transcription factors is involved in many important normal cellular events such as cell-cycle progression, self-renewal, and RNA biogenesis, but these proto-oncogenes are also associated with tumor growth and polyploidy in several types of cancer (6). During early nervous system development, *MycN* is excluded from the neural crest stem cell region and instead is expressed in adjacent neural precursors fated to become part of the CNS, whereas its paralogue *cMyc* is endogenously expressed in the neural crest (7). Later during neural development, MycN has been associated with the maintenance of neural fate (8, 9), as it is expressed by slowly proliferating neural stem cells (radial glial progenitor cells) (10), and is required for neural progenitor expansion and differentiation in the CNS (8, 9). In the peripheral nervous system, MycN also promotes neural fate and differentiation (11, 12).

Following neural crest EMT from the CNS, *MycN* is expressed only at very low levels in migrating neural crest cells (9, 13) and appears to be further down-regulated before the cells coalesce to form ganglia. Later, it has been reported to be reexpressed in differentiating sympathetic ganglia after the onset of the expression of proneural genes such as *ASCL1 (MASH1/HASH1)* and lineage-determining factors such as *Phox2B* and *Hand2* (14–21). Some data suggest that the initiation of *MycN* expression in the ganglia is concomitant with *Phox2a* expression, followed by *Gata2/3*, the *Trk* genes, and the noradrenergic enzymes tyrosine hydroxylase (TH) and dopamine beta hydroxylase (DβH) that are associated with

Significance

Neuroblastoma is a neural crest-derived pediatric cancer that develops in the embryonic peripheral nervous system (PNS). Studies of PNS progenitors have failed to uncover how tumors initiate or fully recapitulate the most aggressive forms of the disease. Previous transcriptome analysis reveals similarity between some neuroblastoma samples and neural stem cells. Here, we show that ectopic expression of MycN in the neural crest domain of the developing neural tube biases neural crest stem cells toward a more CNS neural stem cell-like fate and thus results in improperly specified neural crest cells. This may play a role as a priming event for tumor initiation, thus providing useful insights into understanding the mechanism behind neuroblastoma formation.

Author contributions: L.K., P.N., S.M., J.W., and M.E.B. designed research; L.K., P.N., J.H., F.M.V., Z.T., and A.L. performed research; L.K. and S.M. contributed new reagents/analytic tools; L.K., P.N., J.H., S.M., and F.M.V. analyzed data; and L.K., S.M., J.W., and M.E.B. wrote the paper.

Reviewers: A.N., Instituto de Neurociencias de Alicante, Consejo Superior de Investigaciones Científicas-Universidad Miguel Hernández; and C.T.-G., National Institutes of Health.

The authors declare no conflict of interest.

[1]To whom correspondence should be addressed. Email: mbronner@caltech.edu.

This article contains supporting information online at www.pnas.org/lookup/suppl/doi:10.1073/pnas.1800039115/-/DCSupplemental.

Published online July 18, 2018.

terminal differentiation and functionality of sympathetic neurons (22–24), although this remains controversial (9, 25–27). Postnatally, MycN is not expressed in the sympathetic ganglia (16). Importantly, overexpression of MycN in mouse sympathoadrenal progenitors in vivo is not sufficient for tumor formation but instead results in increased neural differentiation (28). However, neuroblastoma-like tumors were reported after enforced MycN expression in migrating neural crest cells (29), suggesting that premature exposure of neural crest cells to high MycN levels may be important for neuroblastoma initiation.

Like MycN, CIP2A (cancerous inhibitor of protein phosphatase 2A) is overexpressed in several cancer types (30–34) and has been shown to play a role during CNS development as well as in the testis (35, 36). Although CIP2A is known to stabilize cMyc by shielding it from protein phosphatase 2A (PP2A)-mediated degradation (37), it has not previously been associated with MycN.

Here, we tackle the potential links between MycN/CIP2A function in early nervous system development and neuroblastoma. In the embryo, we find that both *MycN* and *CIP2A* are coexpressed in the forming CNS. However, upon initiation of *cMyc* expression in the neural crest stem cell domain of the neural tube (7, 13), *CIP2A* shifts and is coexpressed with *cMyc* instead of *MycN*. As in the early embryonic CNS, *MycN* and *CIP2A* are coexpressed in high-risk neuroblastoma. Interestingly, ectopic expression of MycN in the neural crest domain biases neural crest progenitors toward a more CNS-like neural stem cell identity, so that MycN-expressing neural crest cells may lack a normal neural crest identity. Similarly, some neuroblastomas have a transcriptional resemblance to CNS neural stem cells (38). This raises the intriguing possibility of a fate bias from presumptive PNS to more CNS-like cells, leading to improper differentiation of neural crest cells, perhaps contributing to the priming of tumor initiation in neuroblastoma.

Results

Expression Pattern of *CIP2A* Overlaps with *MycN* in the Early Neural Plate and Closing Neural Tube. CIP2A is a known stabilizing factor for cMyc, which is important for neural crest specification (7, 13). However, we found that *CIP2A* expression starts in the developing neural plate (Fig. 1*A*) at the gastrula stage [Hamburger Hamilton (HH) stage 4] and well before the onset of *cMyc* expression, which initiates only at the time of neural tube closure. This prompted us to examine other potential binding partners for CIP2A. Although not previously implicated as a CIP2A-binding partner, in situ hybridization shows that *CIP2A* and *MycN* have very similar expression patterns during the early neurulation stages (Fig. 1*A*), whereas *cMyc* is absent from the neural plate (7, 13). At stage HH7, *CIP2A* and *MycN* are expressed at high levels in the neural plate but are absent from the neural plate border, which will give rise to the neural crest as highlighted by Pax7 immunostaining. As the neural tube closes (starting at stage HH8 in the cranial region), *CIP2A* and *MycN* are coexpressed throughout the neural tube except in the dorsum, where cMyc expression initiates. Finally, at stage HH9, as the cranial neural crest initiates migration, *CIP2A* expression shifts from the neural region to neural crest and is apparent in the premigratory neural crest cells, overlapping with *cMyc*, but is down-regulated in other parts of the neural tube that remain marked by *MycN* expression (Fig. 1 *B* and *C* and *SI Appendix*, Fig. S1*A*). Along the entire body axis, *MycN* and *CIP2A* are expressed in the neural plate and neural tube, whereas *cMyc* expression is absent before the premigratory neural crest stage (*SI Appendix*, Fig. S1*B*). Migrating neural crest cells (stage HH10) express high levels of *cMyc* and *CIP2A* but much lower levels of *MycN* mRNA, which remains strongly expressed in the more ventral parts of the neural tube that will form the CNS. *CIP2A* expression was also detected in the ectoderm at these later stages (Fig. 1 *B* and *C* and *SI Appendix*, Fig. S1*B*). Taken together, the results show that *CIP2A* expression overlaps with *MycN* during early nervous system development before *cMyc* expression but subsequently is coexpressed with *cMyc* in premigratory and migrating neural crest cells.

***MycN* Is Not Expressed in the Forming Peripheral Ganglia.** Since neuroblastoma tumors are typically found in sympathetic and adrenal sites, we next examined the expression pattern of *MycN* at the end of neural crest migration and onset of their condensation into peripheral ganglia. To this end, we performed in situ hybridization using a specific probe that gave strong expression in other parts of the embryo (limb buds, neural plate, neural tube, and others). Despite long exposure times, we failed to detect *MycN* expression either in migrating neural crest cells or condensed dorsal root or sympathetic ganglia (Fig. 2 *A* and *B*) from stage HH12 (equivalent to human ∼E24/week 3.5) to E4 (equivalent to human E40–42/week 6). Similarly at E7 (equivalent to human E50–52/week 7–7.5) the TH^+ sympathetic ganglia did not express *MycN* (Fig. 2 *C* and *D*). These results suggest that *MycN* is largely absent from the peripheral nervous system during the early stages of embryogenesis corresponding to the first trimester in human development.

Effects of the Loss of MycN or CIP2A on Early Nervous System Development and the Neural Crest. To investigate their developmental role, we next performed loss-of-function experiments using translation-blocking morpholinos (Mo) against *CIP2A* or *MycN*. These were electroporated into the epiblast so that a blocking morpholino was introduced on one side of the embryo, and a control morpholino (CoMo) was introduced on the contralateral side as an internal control (*SI Appendix*, Fig. S2*A*). To demonstrate morpholino efficacy, we compared the ability of CIP2AMo or MycNMo versus the control morpholino to block expression of a construct containing the truncated 5′ UTR and ORF, including the morpholino-recognition sequence, of their respective genes driving expression of RFP. Both morpholinos produced efficient and specific loss of the corresponding construct (*SI Appendix*, Fig. S2 *B–D*).

The results show that the loss of CIP2A disrupts the induction and early specification of neural crest cells. Expression of the neural plate border markers *Msx1/2* and Pax7 at stage HH7 was reduced in over 80% of the embryos ($n = 39$) (Fig. 3 *A–C* and *H*). In a transverse section, *Msx1/2* expression was nearly completely missing on the CIP2AMo side of the neural plate border at stage HH7 (Fig. 3 *B* and *B′*). Slightly later in development (stage HH8), expression of the neural crest-specifier gene *FoxD3* was severely reduced, with >90% of embryos displaying a strong phenotype ($n = 12$) (Fig. 3 *E*, *E′*, and *H*) as viewed in whole mounts. In contrast, embryos electroporated with the CoMo alone showed no phenotype and little loss of neural crest marker expression (stage HH7, $n = 19$ and stage HH8, $n = 20$), displaying only normal variation between the two sides (Fig. 3 *A*, *D*, and *H*).

To further demonstrate the specificity of CIP2A knockdowns, we performed rescue experiments. To this end, CIP2A was expressed together with the CIP2A morpholino. We observed a dose-dependent effect, with 88% of the embryos rescued to normal with 1 μg/μL of CIP2A ($n = 8$) (Fig. 4*B* and *SI Appendix*, Fig. S2*E*) and 57% rescued with 0.5 μg/μL ($n = 7$).

Next we examined the effects of the loss of MycN, a member of the Myc family that is expressed in in the neural plate (the future CNS) in a similar fashion to CIP2A. Similar to the loss of CIP2A, the loss of MycN also caused a deficit of neural crest precursors at the neural plate border (stage HH7, $n = 39$) as shown in a transverse section (Fig. 3 *F* and *H*). Slightly later, when the neural tube is closed (stage HH8, $n = 37$), the expression of *FoxD3* in premigratory neural crest cells in the dorsal neural tube was clearly affected also (Fig. 3 *G* and *H*; stage HH7: 67% strong, 28% mild, and 5% no phenotype; stage HH8: 82% strong, 5% mild, and 11% no phenotype). The phenotype was penetrant throughout the embryo from cranial to trunk levels. These results suggest that knockdown of both MycN and CIP2A impacts neural crest development although neither gene is expressed in the presumptive

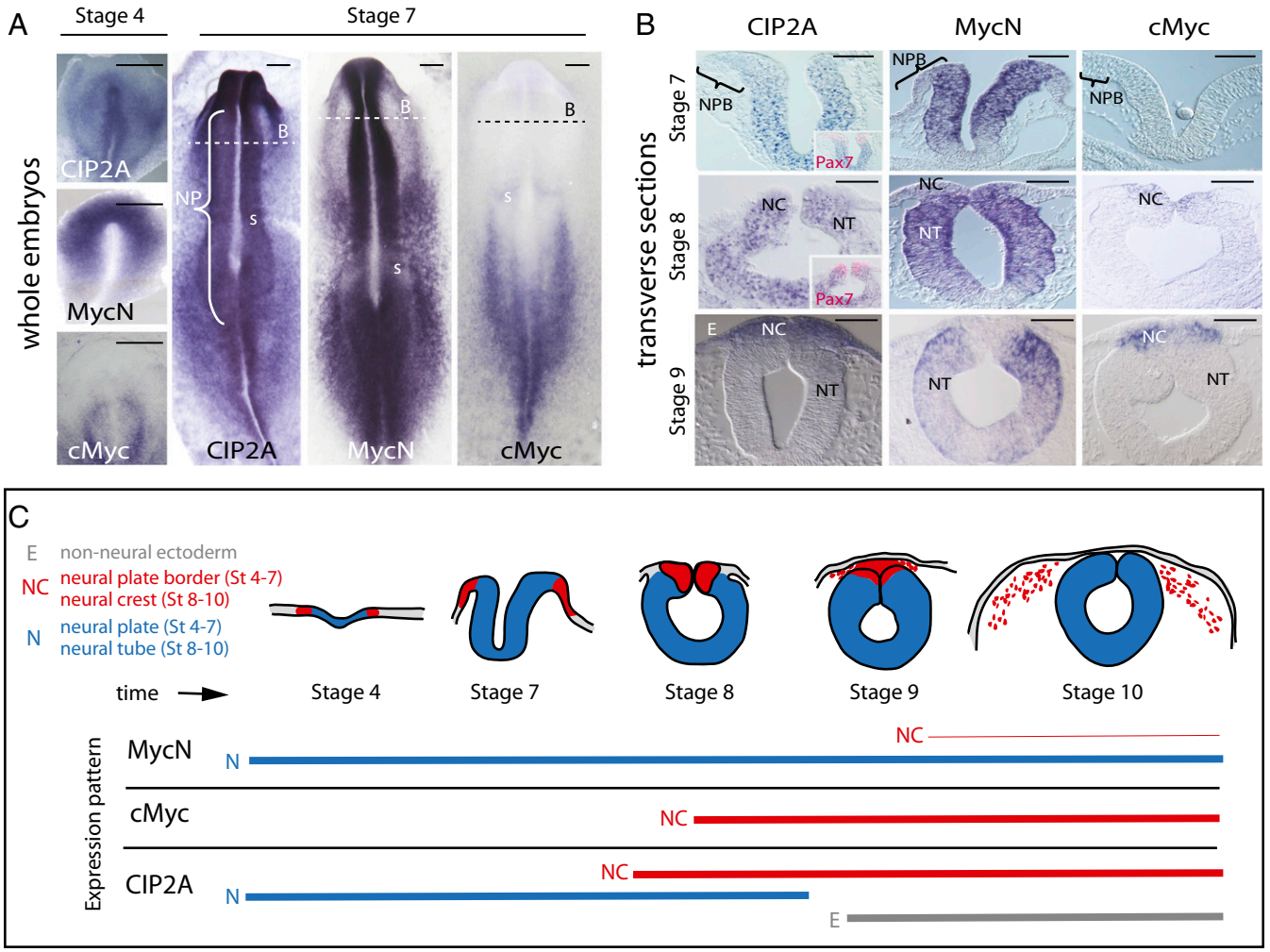

Fig. 1. Expression patterns of *CIP2A*, *MycN*, and *cMyc* in the developing neural tube and neural crest cells in the chicken embryo. (*A*) Whole-mount in situ hybridization shows that *CIP2A* and *MycN*, but not *cMyc*, are expressed in the neural plate (NP) during gastrulation throughout the anterior-to-posterior axis. B, areas shown in panel *B*; s, somites. (*B*) In contrast, the neural plate border (NPB) that later forms the neural crest does not express any of the three genes at stages HH4–7 as also seen in transverse sections. As the neural tube closure begins at stage HH8, *CIP2A* is expressed throughout the entire neural tube (NT), whereas *MycN* is restricted to the ventral parts that will form the CNS. *cMyc* expression onsets at late stage HH8 in the dorsal neural tube that will become the neural crest (NC). By stage HH9 *CIP2A* and *cMyc* are restricted to the dorsal neural crest area, whereas *MycN* is expressed in the remaining neural tube but not in the dorsum. *CIP2A* expression is also seen in the nonneural ectoderm (E) after stage HH9. (Scale bars: 20 μm.) (*C*) A schematic diagram summarizing the expression patterns seen in *A* and *B* and *SI Appendix*, Fig. S1. Red represents the neural crest, blue represents neural stem cells of the future CNS, and gray is future epidermis. The thin red line for *MycN* represents a much lower expression level of *MycN* in the migrating neural crest compared with the other stages and genes, respectively.

neural crest at this early developmental time point. Thus, we speculate that both MycN and CIP2A are required for proper development of the neural plate and thus the neural stem cells that form the CNS, and that disruption of this process secondarily affects subsequent neural crest development in the neural plate border (39).

Epistatic Relationship Between MycN and CIP2A. To examine whether CIP2A and MycN may be functionally associated, we asked whether the loss of CIP2A, predicted to lead to faster degradation of MycN, can be compensated by the overexpression of MycN. To this end, we knocked down CIP2A using a morpholino and coinjected MycN to test whether this was sufficient to rescue the phenotype. Indeed, 75% of the embryos ($n = 12$) were rescued by coinjection of 0.75 or 1 μg/μL MycN (Fig. 4 *A*, *A′*, and *B*) and 62% ($n = 4$) were rescued with 0.5 μg/μL MycN. Interestingly, a small percentage (<20%) of the embryos showed a slight increase in the expression of the neural crest marker *FoxD3* (Fig. 4*B*). These results reveal a dose-dependent ability of MycN to rescue the effects of loss of CIP2A, consistent with an epistatic interaction.

Ectopic MycN or CIP2A Causes a Shift in Neural Crest Identity Toward a More CNS-Like Fate. Since amplification of MycN is a hallmark of neuroblastoma with poor prognosis, we next examined the effects of elevated MycN or CIP2A in the neural plate border and presumptive neural crest domain, sites where MycN is not endogenously expressed. The results show that overexpression of either CIP2A or MycN significantly reduced the expression of neural crest markers *FoxD3* and Pax7 at all axial levels from cranial to anterior trunk (Fig. 5 *A*, *B*, and *D*). Instead, ectopic MycN in the dorsal neural folds led to enhanced CNS stem cell identity as shown by increased Sox2 throughout the neural tube (from ventral to dorsal, Fig. 5 *C* and *D*, and "Sox2 all" in Fig. 5*G*).

Importantly, the neural crest domain, as indicated by the expression of Pax7, was significantly reduced in size, suggesting that ectopic MycN may have neuralized a large proportion of the cells

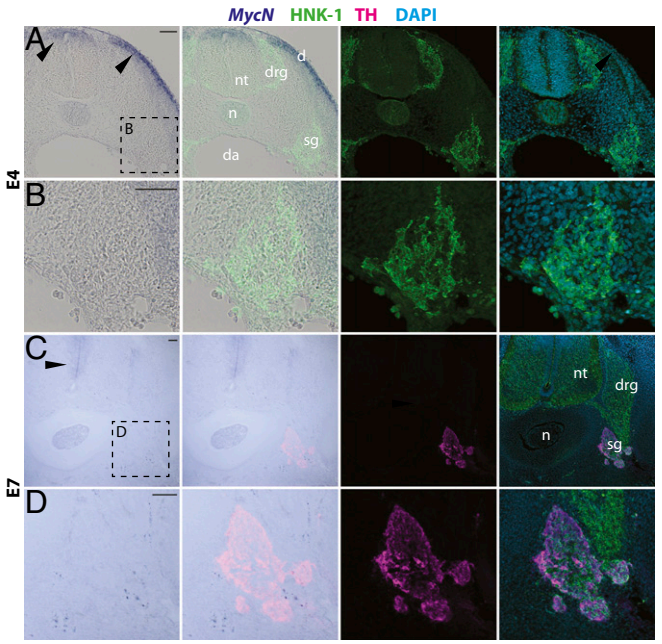

Fig. 2. *MycN* is not expressed in the developing sympathetic ganglia. (*A*) At day 4 of chicken embryo development, *MycN* is expressed in the dorsal neural tube and the dermatome (arrowheads), but no *MycN* expression was detected in the peripheral ganglia as shown by in situ hybridization in the trunk level. The ganglia are highlighted by HNK immunostaining. (*B*) High-magnification images of the E4 sympathetic ganglia with no *MycN* expression. (*C*) At day 7, *MycN* expression is visible in the ventricular apical region surrounding the neural tube, but no expression is detected in the TH-immunopositive sympathetic ganglion. (*D*) High magnification of the E7 sympathetic ganglia with no *MycN* expression (boxed area in panel *C*). d, dermatome; da, dorsal aorta; drg, dorsal root ganglion; n, notochord; nt, neural tube; sg, sympathetic ganglion. (Scale bars: 100 μm.)

in the neural crest domain (green arrowheads in Fig. 5*E*), as also shown by a decrease in overall Pax7 expression on the MycN-injected side compared with control embryos (Fig. 5*G*). Consistent with this possibility, even the small remaining population of Pax7$^+$ neural crest cells had significantly higher Sox2 levels compared with the endogenous Sox2 expression levels on the control side (Fig. 5*E* and "Sox2 dorsal" in Fig. 5*G*).

Although very low Sox2 levels are normally present in neural crest cells (see control side in Fig. 5*E*), quantitative analysis at single-cell-level resolution revealed a significant increase in the cells that expressed high or intermediate levels of Sox2 in the MycN-overexpressing neural crest domain. Conversely, the number of cells that express no or low levels of Sox2 (normally 75% of the neural crest cells) was reduced to 45% due to enhanced MycN expression (see pink arrowheads indicating high Sox2 levels and purple arrowheads indicating intermediate Sox2 levels in Fig. 5*E* and quantifications in Fig. 5*H*). Ectopic MycN also caused a significant decrease in the proportion of Sox2$^-$ cells [from 42% (SD = 0.06) on the control side to 20% (SD = 0.1) on the MycN-injected side; $P = 0.003$, $n = 7$], consistent with an overall increase in Sox2 levels on the MycN-injected side (Fig. 5*G*). In contrast, the Pax7 levels in individual cells were decreased by 25% on average (Fig. 5*I*) but displayed less variance (ranging from medium to high levels) than Sox2 expression on both the MycN-overexpressing and the control sides (Fig. 5*E*). Cells expressing both high Pax7 and high Sox2 levels on the control side were extremely rare, with only a few found at the border region between CNS and neural crest domains in seven embryos; this number was significantly (14-fold) higher following MycN overexpression (Fig. 5*J*). These results suggest that ectopic MycN shifts the presumptive neural crest domain toward a more CNS-like neural stem cell fate. This is consistent with reports showing that fate changes can occur by tweaking transcription factor levels in the neural plate border (40). Importantly, these results suggest that the abnormally high levels of Sox2 do not abolish neural crest identity but rather result in a mixed identity (high/intermediate Sox2$^+$/Pax7$^+$), which we refer to as "CNS-like" neural crest cells.

CNS-Like Neural Crest Cells Emigrate from the Neural Tube and Are Migratory. The results described above raised the intriguing question of whether these Sox2$^+$/Pax7$^+$ CNS-like neural crest cells can undergo EMT, migrate, and contribute to the peripheral nervous system. To address this possibility, we examined embryos at later times, when neural crest cells were emigrating and migrating through the periphery. The results showed that neural crest cells with excess MycN were able to undergo EMT to leave the CNS. Although some migrating MycN-overexpressing cells lacked Pax7, perhaps reflecting bias toward a neural fate (Fig. 5*F*,

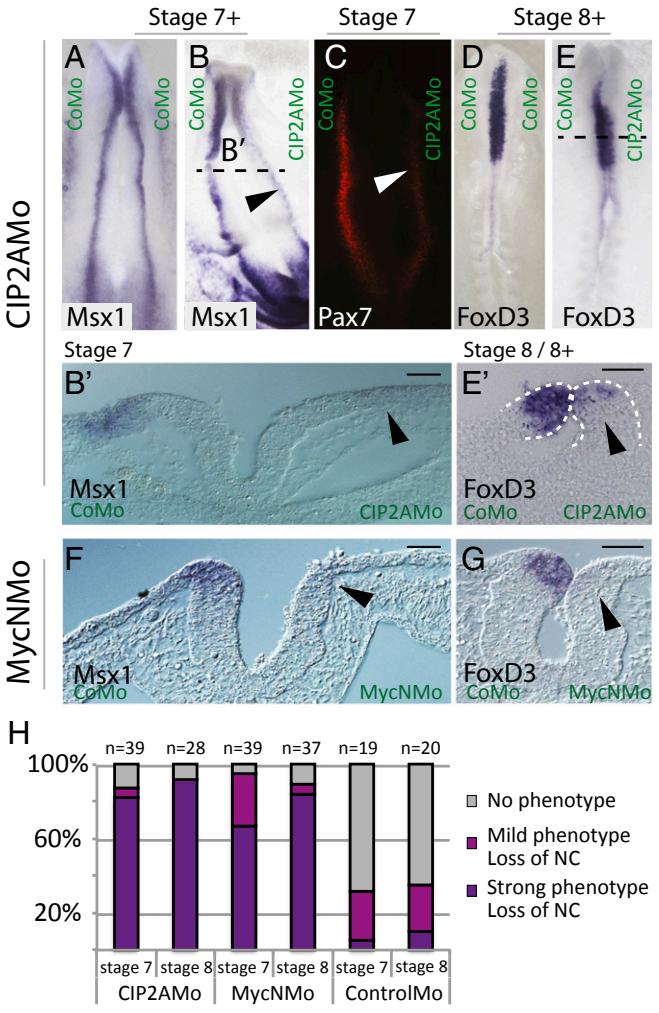

Fig. 3. Neural crest is lost upon knockdown of MycN or CIP2A. (*A*–*C*) Whole-mount images of a chicken embryo electroporated with a control morpholino shows similar expression of the neural plate border marker *Msx1* on both sides (*A*), while knockdown of CIP2A significantly reduces the expression of both *Msx1* (*B* and *B*′) and Pax7 (*C*) along the entire neural axis of the embryo at stage HH7 (arrowheads). (*D*–*E*′) The phenotype persists at stage HH8, as expression of the neural crest specifier gene *FoxD3* is reduced from anterior to posterior parts of the embryo. (*F* and *G*) Similarly, morpholino-mediated knockdown of MycN causes a loss of the expression of *Msx-1* (*F*) and *FoxD3* (*G*). (Scale bars: 20 μm.) (*H*) Quantification of the phenotypes.

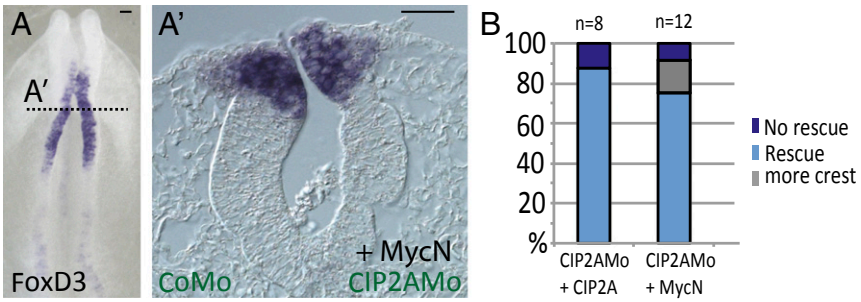

Fig. 4. CIP2A and MycN cooperate in the developing neural tube. (*A* and *A′*) Loss of CIP2A is rescued by coexpression of MycN as shown by whole-mount in situ hybridization for *FoxD3* (*A*) and in a transverse section of the same embryo (*A′*). (Scale bars: 20 μm.) (*B*) Quantification of the rescue experiments.

blue arrowheads), most remained Pax7$^+$ (Fig. 5*F*, white arrowheads). In addition, there was variability in the MycN-RFP levels, with some cells expressing high levels of Pax7 having low MycN-RFP expression (Fig. 5*F*, pink arrowheads). This is expected, since the expression levels of constructs are variable from cell to cell after electroporation.

In line with the premigratory stages (Fig. 5 *D* and *E*), shortly after emigration we noted fewer migrating neural crest cells (n = 3) (*SI Appendix*, Fig. S2*F*). With time, however, the numbers of the neural crest cells observed migrating further laterally increased (Fig. 5 *F* and *K*). Immunostaining showed that migrating MycN-overexpressing neural crest cells had lost their Sox2 expression (*SI Appendix*, Fig. S2*F*), in accordance with previous reports (40, 41). These results suggest that the CNS-like Pax7$^+$/MycN$^+$ neural crest cells are able to undergo EMT and that migrating MycN-overexpressing cells matured from Sox2$^+$ precursors into peripheral nervous system progenitors. This is consistent with previous experiments showing that overexpression of MycN at the migratory stage causes an excess of neural crest cells that predominantly differentiate into peripheral neurons (11).

Strong Association of High *MycN* and *CIP2A* Levels with Aggressive Forms of Neuroblastoma. Next, we asked whether the scenario functioning during early neural plate and neural crest development might be recapitulated in neuroblastoma. To this end, we examined potential correlations between the expression of *CIP2A*, *MycN*, and *cMyc* in neuroblastoma samples using three independent datasets: KOCAK (Fig. 6), SEQC498 (*SI Appendix*, Fig. S3), and Versteeg88 (*SI Appendix*, Fig. S4).

All three datasets display substantial mRNA expression levels of all three transcripts, although the *MycN* levels were in the highest range (Fig. 6*A* and *SI Appendix*, Fig. S4*A*). The expression pattern for *MycN* was bimodal, presumably reflecting *MycN*-amplified versus nonamplified status: In the first group, the majority of samples had lower expression levels, ranging from $2\log^{12}$ to $2\log^{15}$, whereas in the second group the levels ranged from $2\log^{15}$ to $2\log^{18}$. Expression levels of *cMyc* were in the range between $2\log^{11}$ and $2\log^{15}$ and were lowest for *CIP2A*, ranging from $2\log^{7}$ to $2\log^{12}$ (Fig. 6*A*). When the expression levels of *MycN* were compared in the MycN-amplified versus the nonamplified group, the results clearly show that the levels in the nonamplified group are comparable to *cMyc* levels, and thus the levels were much higher in the MycN-amplified tumors (Fig. 6*B*). As in the early embryo (Fig. 1), the expressions of the two *Myc* family members show a strong inverse correlation (Fig. 6*C* and *SI Appendix*, Fig. S3*A*), suggesting that they are not likely to be coexpressed in the same neuroblastoma tumors. However, *MycN* and *CIP2A* mRNA expressions show positive correlation in the complete dataset as well as in stage 4 tumors only, reminiscent of the situation we observe in the early embryo (Fig. 5) after ectopic MycN expression in the neural crest domain (Fig. 6*D* and *SI Appendix*, Figs. S3*B* and S4*B*). However, although this correlation is maintained in both the MycN-amplified and nonamplified stage 4 tumors in the SEQC498 dataset (*SI Appendix*, Fig. S3*B*), it is lost in the MycN-amplified cases in the KOCAK dataset (Fig. 6*E*), suggesting a stronger correlation with the "more physiological" MycN expression levels (Fig. 6*B*). Conversely, expression of *cMyc* and *CIP2A* correlated negatively in the KOCAK dataset as well as in stage 4 tumors only; however, their expression was weaker in the MycN-nonamplified stage 4 tumors (Fig. 6*F*), whereas their correlation was weaker in the complete dataset and was lost in stage 4 tumors in the SEQC498 dataset (*SI Appendix*, Fig. S3*D*). The number of individual tumors in the MycN-amplified and/or the stage 4 group is low (even in the largest KOCAK dataset there are 41 and 65 tumors, respectively). Thus, the sample size may be too low for statistical significance or for drawing firm conclusions. In line with the other datasets, in the Versteeg88 dataset *CIP2A* correlates with *MycN* in the MycN-nonamplified group (*SI Appendix*, Fig. S4*B*) and correlates negatively with cMyc in the MycN-amplified group (*SI Appendix*, Fig. S4*C*). We also found that *MycN* (as previously known) and *CIP2A* individually correlate significantly with the International Neuroblastoma Staging System (INSS) stages, i.e., highest expression is found in the most aggressive stage 4 tumors, whereas *cMyc* shows an opposite declining trend (Fig. 6*G* and *SI Appendix*, Figs. S3*C* and S4*E*).

Consistent with previously published results, high expression of both *MycN* (3, 4) and *CIP2A* (42) correlate with poor prognosis in neuroblastoma in all three clinical datasets analyzed here (Fig. 6 *H* and *J* and *SI Appendix*, Figs. S3 *E* and *G* and S4*D*). However, the correlation between CIP2A and outcome is significant only in the complete dataset and in the MycN-nonamplified tumors but is lost in the MycN-amplified tumors and stage 4 tumors (Fig. 6*H* and *SI Appendix*, Fig. S3*E*). In contrast, expression of *cMyc* was associated with improved patient survival in both the complete dataset and stage 4 tumors (Fig. 6*I* and *SI Appendix*, Fig. S3*F*) and thus shows an inverse correlation compared with its ortholog *MycN* (Fig. 6*J* and *SI Appendix*, Fig. S3*G*). Together, these results are consistent with functional cooperation between MycN and CIP2A in the development of clinical neuroblastoma.

CIP2A Promotes SOX2 Expression in MycN-Amplified Neuroblastoma Cells. To further explore the functional relationship of MycN and CIP2A in neuroblastoma, we utilized a panel of neuroblastoma cell lines with [SK-N-BE(2); NGP cells] or without (SK-N-AS cells) MycN amplification. Both MycN-amplified neuroblastoma cell lines were positive for CIP2A and Sox2 but expressed very low or undetectable levels of cMyc (Fig. 7*A*). Instead, SK-N-AS cells that harbor normal MycN copy numbers expressed extremely low protein levels for both MycN and Sox2 but expressed substantial levels of cMyc (Fig. 7*B*). This reciprocal relationship between cMyc and MycN is reminiscent of our observations in the dorsal neural tube of early embryos (Fig. 1) as well as in clinical neuroblastoma (Fig. 6).

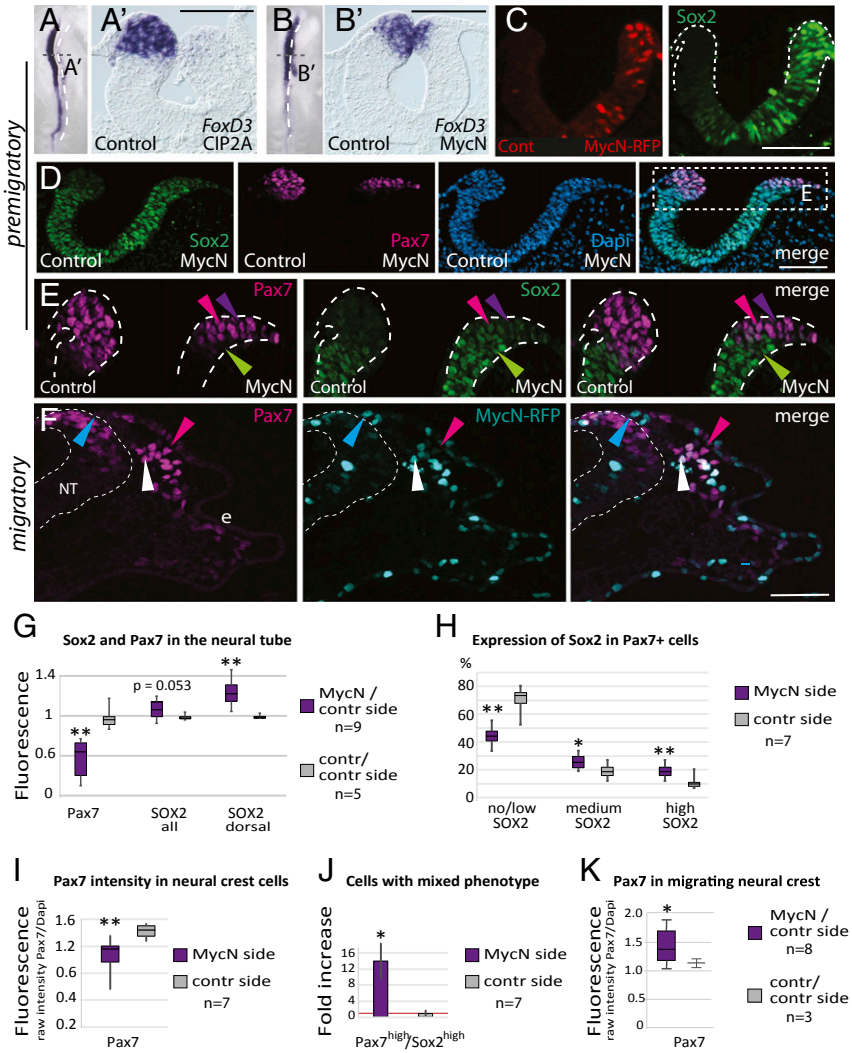

Fig. 5. Enhanced MycN in the neural crest domain causes a fate bias toward CNS-like neural stem cells. (*A*–*B*′) Ectopic expression of either CIP2A (*A* and *A*′) or MycN (*B* and *B*′) leads to a significant decrease in the size of the neural crest domain as shown by in situ hybridization for *FoxD3*. (*C*) Electroporation of MycN-RFP causes an increase in Sox2 protein levels throughout the neural folds. (*D*) This leads to both full and partial neuralization of the $Pax7^+$ neural crest domain. (*E*) Enlarged view of the boxed area in *D* highlights the different levels of neuralization due to ectopic MycN: completely neuralized $Sox2^+/Pax7^-$ cells (green arrowheads), partially neuralized $Pax7^{high}/Sox2^{high}$ cells (pink arrowheads), and $Pax7^{high}/Sox2^{intermediate}$ cells (purple arrowheads). (*F*) Neural crest cells are able to emigrate and migrate despite ectopic MycN, and most of the cells also express Pax7 (white arrowheads), while some are $MycN^+/Pax7^-$ (blue arrowheads). Electroporation causes variability as shown by a lower MycN level in some cells (pink arrowheads). e, ectoderm; NT, neural tube. (*G*) Pax7 expression is significantly decreased on the MycN ectopic side ($P = 0.0041$; *t* test), reflecting the smaller size of the neural crest domain, and $Sox2^+$ levels are increased both in the entire neural tube (Sox2 all), and the neural crest domain (Sox2 dorsal) ($P = 0.0021$). (*H*) Ectopic MycN increases Sox2 levels in $Pax7^+$ neural crest cells (high, $P = 8.6E\text{-}06$; medium, $P = 0.042$; *t* test). Conversely, the proportion of normal neural crest cells with no or low Sox2 levels was reduced from 75 to 45% ($P = 7.4E\text{-}05$; *t* test) on the MycN-injected side (*I*), and Pax7 expression decreased by 25% ($P = 0.0031$; *t* test). (*J*) The number of cells with high levels of both Pax7 and Sox2 is increased by 14-fold ($P = 0.011$; *t* test). (*K*) The MycN-overexpressing side has more $Pax7^+$ migratory neural crest cells than the control side. The lines inside the box plots represent the median values. (Scale bars: 50 μm.) $*P < 0.05$, $**P < 0.01$.

To test for a possible direct interaction between CIP2A and MycN, we used the proximity ligation assay (PLA) to examine the physical proximity of these proteins in the SK-N-BE(2) cell line. The results show that CIP2A and MycN indeed associate with each other (Fig. 7*C*).

We next addressed whether the in vivo cooperation between CIP2A and MycN in the regulation of Sox2 expression shown in avian embryos (Fig. 5) was a cell-autonomous process. To this end, we tested the effects of CIP2A depletion in neuroblastoma cells using three independent siRNAs. CIP2A depletion caused changes in cellular responses in a cell-viability assay (Fig. 7*D*), with cells exhibiting decreased anchorage-independent growth in a soft agar assay (Fig. 7*E*). Importantly, CIP2A depletion significantly reduced Sox2 protein expression in the MycN-amplified cell lines, consistent with the in vivo results. Levels of MycN were slightly increased, possibly due to a compensatory effect caused by a lack of the normal half-life protected by CIP2A (Fig. 7*A*). Interestingly, in the MycN wild-type cells that display a more neural crest-like expression profile (low levels of Sox2/MycN and physiological levels of cMyc), the loss of CIP2A had no effect on cMyc (Fig. 7*B*), further suggesting that CIP2A expression in neuroblastoma is connected to MycN and not to cMyc. These results suggest that the cooperation of MycN and CIP2A in Sox2 regulation observed both in vivo and in vitro is cell autonomous. They also confirm that the molecular features detected in neuroblastoma cells and in clinical neuroblastoma are similar to those observed during early CNS development.

Finally, we tested whether *Sox2* and *MycN* correlate in clinical neuroblastoma. The expression levels of *Sox2* in the KOCAK and

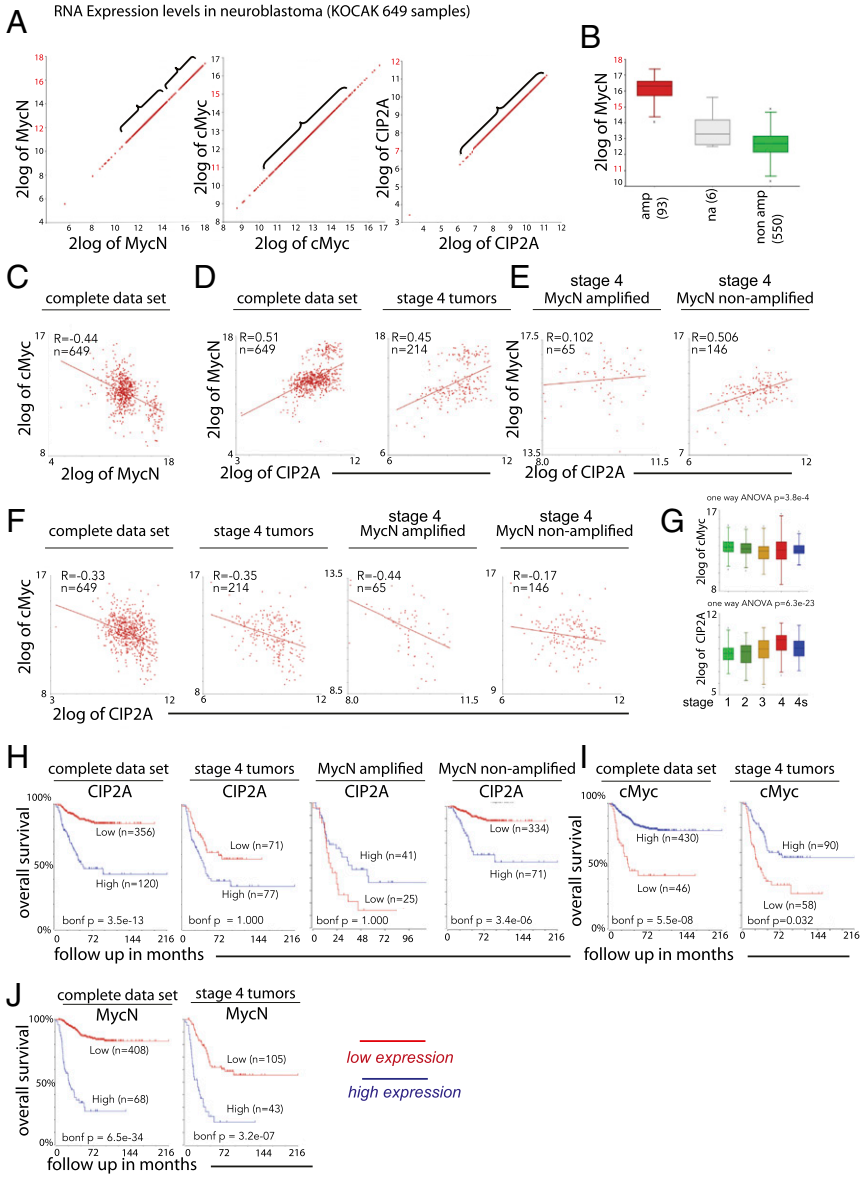

Fig. 6. CIP2A and MycN are strongly correlated with a poor prognosis, while cMyc correlates with better survival probability. (*A*) MycN, cMyc, and CIP2A show substantial expression levels in neuroblastoma with CIP2A displaying the lowest range. The expression of MycN is bimodal, and the expression in the highest group exceeds the level of *cMyc* and *CIP2A*. Note the different values on the *x* and *y* axes in each image. (*B*) The bimodal expression of *MycN* mRNA in MycN-amplified (amp) and nonamplified (non amp) tumors shows how the amplified levels are above physiological levels. (*C*–*E*) Expression of *cMyc* and *MycN* shows negative correlation in clinical neuroblastoma samples (*C*), whereas *MycN* correlates positively with *CIP2A*, as shown both in the complete dataset and in stage 4 tumors only (*D*), but, presumably due to the extremely high expression levels, the correlation is lost in the MycN-amplified stage 4 tumors, whereas strong correlation is shown in the stage 4 nonamplified group (*E*). (*F*) *CIP2A* and *cMyc* correlate negatively in the complete dataset and stage 4 tumors, but the correlation is weaker in the MycN-nonamplified stage 4 tumors. (*G*) *CIP2A* expression correlates significantly with the INSS stage, and *cMyc* shows an inverse correlation. (*H*) Kaplan–Meier curves showing a significantly lower survival probability for patients with high *CIP2A* levels in the complete dataset and in MycN-nonamplified tumors (with more physiological *MycN* expression levels). The correlation is lost in the stage 4 tumors and in the MycN-amplified group. (*I* and *J*) High *cMyc* expression levels (which may represent physiological rather than overexpressed levels) correlate with better survival probability in clinical neuroblastoma in both the complete and stage 4 datasets (*I*), whereas *MycN*, as previously known, correlates with a poor outcome (*J*). $*P < 0.05$; na, not available.

SEQC498 clinical datasets were low, with the majority of the tumors ranging from $2\log^5$ to $2\log^9$, and there is no significant correlation with *MycN* (*SI Appendix*, Fig. S5 *A* and *B*). This is in line with our finding that Sox2 levels are down-regulated after emigration from the neural tube during normal development and in MycN-overexpressing neural crest cells (*SI Appendix*, Fig. S2*F*). We also tested whether we could detect a correlation between *MycN* and other commonly known neural stem cells markers such as *Nestin* or *Mushashi2*, but no significant correlations were noted (*SI Appendix*, Fig. S5 *C*–*F*). These results suggest that the expression of Sox2 in neuroblastoma cell lines may be a sign of regression into an earlier developmental time point that is not maintained in tumors in vivo but exists under certain culture conditions in vitro.

Discussion

Despite extensive efforts and different forms of therapy, treatment of aggressive high-risk neuroblastoma remains a challenge.

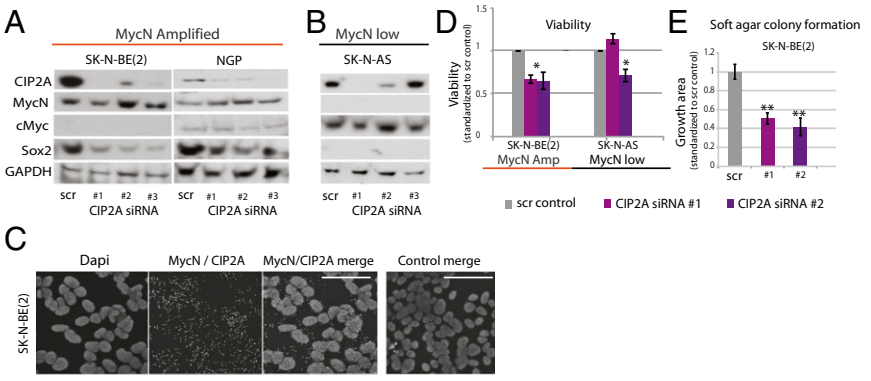

Fig. 7. Loss of CIP2A impacts proliferation and anchorage-dependent growth. (*A*) Knockdown of CIP2A with three different siRNAs reduces the expression of Sox2 in MycN-amplified neuroblastoma cell lines. (*B*) SK-N-AS cells with wild-type MycN status express undetectable levels of MycN or Sox2 but substantial levels of cMyc that are unaffected by the knockdown of CIP2A. (*C*) The PLA shows cobinding of MycN and CIP2A. (Scale bars: 50 μm.) (*D*) Knockdown of CIP2A reduces relative viability in neuroblastoma cell lines [SK-N-BE(2), $P = 0.00040$ and 0.01201; SK-N-AS, $P = 0.019$, *t* test]. (*E*) Loss of CIP2A also decreased anchorage-dependent growth in SK-N-BE(2) cells ($P = 0.0049$ and 0.0068). $*P < 0.05$, $**P < 0.01$.

Therefore, understanding the initial steps of tumor formation is crucial for designing novel approaches for treatment. Neuroblastoma originates in neural crest-derived sympathetic nerves and is associated with reduced neural differentiation capacity and thus an enhanced stem cell-like profile. The etiology remains unknown, and it is likely that multiple mechanisms lead to the heterogeneous group of tumors classified as neuroblastoma. Interestingly, a transcriptome analysis performed over a decade ago reveals that some neuroblastomas have twice as many genes in common with CNS neural stem cells than do normal sympathoadrenal progenitors (38). Since cancer cells often express features that mirror their stem cell origin, this raises the intriguing possibility that factors that might bias neural crest cells toward a more CNS-like state may play a role as a priming event in neuroblastoma. During nervous system development, CNS and PNS precursors arise in adjacent domains within the forming neural plate, with neural crest stem cells in the neural plate border and CNS precursors in the immediately lateral neural plate domain. This led us to investigate whether misregulation of the events that guide fate determination at the neural plate border could help explain the initiation mechanism underlying neuroblastoma formation.

The majority of studies on neuroblastoma initiation to date have focused on finding links to sympathetic ganglia formation. In contrast, far less attention has been paid to the possibility that predisposing oncogenic changes in the premigratory and early migrating neural crest may occur before the cells have migrated to the site of sympathetic ganglia formation. This prompted us to test the hypothesis that the initiation of some forms of neuroblastoma may occur at early time points in nervous system development and well before specification of the sympathoadrenal lineage. Given that the great majority of neuroblastoma research is done in neuroblastoma cell lines that already are malignant, the initial mechanism(s) that triggered the disease may be masked under a series of secondary defects. Therefore, we went back to the early embryo to test the role of both endogenous and ectopic MycN and CIP2A as possible priming factors.

Amplification of MycN remains the strongest single indicator of poor prognosis in neuroblastoma (43). Previously, the developmental role of MycN has been examined primarily at later stages, during neural crest migration and gangliogenesis. In the spinal ganglia and the developing CNS, MycN promotes neural fate and differentiation (8, 9). Overexpression of MycN in migrating neural crest cells of chicken embryos increases the proportion of neurons at the expense of other derivatives (11). Reciprocally, loss of MycN in mouse embryos reduces the size of the entire nervous system, including peripheral, spinal, and cranial ganglia (12), and decreases the number of mature neurons in the spinal ganglia (9). Although it has been assumed that *MycN* was expressed in chick and mouse peripheral ganglia during their formation and maturation (9, 21, 25, 26), we were not able to detect any *MycN* mRNA in the chick sympathetic ganglia at any time point from migratory stages to late gangliogenesis (E2–E7 corresponding to E50–52/week 7–7.5 in humans as the latest time point) (Fig. 2). In contrast to our results, a previous study proposes that there is weak *MycN* expression in sympathetic ganglia. However, they also find strong expression of *cMyc* at the same stage in sympathetic ganglia (25), in line with previous findings (10) and our results here regarding the reciprocal expression pattern of these two orthologs in the embryo and in neuroblastoma. We cannot rule out the possibility that *MycN* is turned on in the sympathetic ganglia later in gestation and then is turned off again before birth. Taking the data together, we speculate that MycN expression in neuroblastoma is ectopic and may reflect an abnormal priming of the early neural crest toward a more CNS-like neural stem cell fate.

While MycN overexpression in sympathoadrenal progenitors in vitro leads to neural lineage commitment and tumor-like characteristics, the onset of this oncogenic program is inhibited in an in vivo context (28). In contrast, MycN overexpression in migrating neural crest cells is sufficient for in vivo transformation and formation of tumors with phenotypic resemblance to neuroblastoma (29), again suggesting that time points before sympathoadrenal lineage specification may be the root of some forms of neuroblastoma. We find that MycN amplification in premigratory neural crest stem cells within the neural tube biases them toward $Sox2^+$ neural stem cells (Fig. 5). While some cells are completely ventralized, losing Pax7 expression, others coexpress high Sox2 levels while retaining Pax7. We hypothesize that these cells may be "primed" for neuroblastoma formation, as they retain the ability to undergo EMT and migrate despite their ectopic CNS-like neural stem cell bias. We speculate that the retention of high MycN levels in the migrating neural crest cells may abnormally induce proliferation and the maintenance of neural identity but that these cells are unable to differentiate normally when they reach the ganglia due to their neural progenitor state.

We report an interesting reciprocal relationship between *cMyc* in the neural crest domain and *MycN* in the remaining neural tube. Although we have shown that cMyc expression is critical for the maintenance of early neural crest identity and self-renewal capacity (Fig. 1) (7, 44), MycN seems to function primarily in CNS neural stem cells. Similarly, we show that the expression of *cMyc* and *MycN* in clinical neuroblastoma (Fig. 6) is complementary in a

manner paralleling that in the embryo (Fig. 1). Our results using a combination of functional studies in the embryo (Fig. 5) together with neuroblastoma cell lines (Fig. 7) and publicly available tumor datasets (Fig. 6 and *SI Appendix*, Figs. S3 and S4) suggest that MycN overexpression (or in many cases amplification) biases their fate from neural crest toward CNS-like neural stem cells and that this bias reflects an early developmental event. The fact that CIP2A partners with MycN only during the early neural plate stage and not later after neural tube closure or in the migrating neural crest cells further strengthens our hypothesis that some tumors are primed at an early developmental time point. It is intriguing to speculate that this early mechanism may reflect the underlying cause of initiation of the most aggressive forms of neuroblastoma. Our findings also bring neuroblastoma closer to other pediatric CNS tumors such as medulloblastoma, raising the possibility that common mechanisms may underlie the initiation of these tumors.

Many pediatric malignancies arise from embryonic cell types that have persisted and give rise to tumors in early childhood (45). Pediatric tumors are thus unlikely to be driven by the gradual accumulation of genetic lesions but rather via oncogenic cells that are predisposed to malignant growth while carrying few mutations (46). In *Drosophila*, it has been shown that intermediate neural progenitors born during a particular time period are predisposed to malignancy (47). Similarly, we speculate here that, rather than immediately initiating rapid tumor growth, these early events may serve as a priming event for tumor susceptibility so that cells ectopically exposed to high MycN levels early in development have the potential for metastatic tumor growth later during ganglia formation.

Neuroblast hyperplasia is detected in normal ganglia before and around birth. Some of these neuroblasts progress into neuroblastoma-like tumors upon MycN overexpression under the TH promoter (45) but do not fully recapitulate the metastatic disease. It is intriguing to speculate that perhaps, in addition to the constitutive ectopic MycN expression in the developing ganglia, the early priming event in the neural plate border we describe in this study triggers the formation of a full-blown metastatic neuroblastoma. This also suggests that existing mouse and zebrafish neuroblastoma models that activate MycN in the peripheral ganglia may initiate the expression at a time point that is too late for understanding the initiation of at least some subgroups of the disease (45, 48–52). Finally, neuroblastoma occasionally occurs in association with other neural crest-derived defects (also known as "neurocristopathies") such as Hirschsprung's disease (53–56), which results from a failure of neural crest cells to populate the most distal portions of the intestines. This supports the idea that early onset of neuroblastoma may occur in multipotent neural crest stem cells before their migration into respective target tissues and perhaps may limit the pool of migrating cells.

We were intrigued by the fact that CIP2A is known to stabilize cMyc, but little was known about its interaction with MycN. We noted that *CIP2A* was expressed throughout the neural plate and neural tube at a time when *cMyc* is not yet expressed. This prompted us to study whether CIP2A might initially stabilize MycN at early times until cMyc is turned on, and indeed, our study reveals CIP2A as a binding partner of MycN (Figs. 4 and 7). CIP2A has an established role as an oncogene, and its knockdown leads to down-regulation of several oncogenic drivers (Akt, cMyc, and E2F1) due to PP2A dephosphorylation-mediated degradation (57). Although the loss of CIP2A does not compromise mouse viability, it causes defects in neural and spermatogonial progenitors (35, 36). Here we show that it is, in collaboration with MycN, also required for the correct formation of the neural stem cell characteristics of the neuroectoderm at the neural plate but not later, after neural tube closure (Figs. 2–4). We also show that CIP2A couples with MycN in neuroblastoma (Figs. 6 and 7), which suggests that this early developmental role is maintained in neuroblastoma. CIP2A is overexpressed in a large fraction of all major human cancer types and, in line with previous findings (37, 57), its inhibition leads to decreased tumor cell viability in neuroblastoma cell lines (Fig. 7), suggesting that CIP2A may be a potential target for neuroblastoma therapy.

cMyc is famous for its oncogenic properties and is overexpressed in multiple cancer types (58). Thus, it is counterintuitive that its expression is associated with higher survival rates and good prognosis in neuroblastoma (Fig. 6). There are several possible explanations for this observation. First, cMyc in neuroblastoma may reflect a more normal multipotent neural crest stem cell state that is capable of responding to cues from the environment to promote differentiation (7). Second, the overall expression levels of *cMyc* in neuroblastoma samples are significantly lower than the expression levels of *MycN* in the MycN-amplified tumors (Fig. 6) and thus are likely to be similar to the endogenous physiological levels during embryonic development. This is in line with the reports on high *cMyc* levels as a prognostic marker for the poor outcome in a small percentage of the undifferentiated subtype of neuroblastoma, NBUD (59, 60), in which the overexpression of cMyc may have triggered the highly proliferative oncogenic machinery that is not turned on in neural crest cells during normal development (7). In line with this, a recent study shows that a subset of high-risk neuroblastomas display upregulated *cMyc* due to enhancer hijacking, and overexpression of cMyc under the DβH promoter induced tumor mass growth in vivo in zebrafish (61). cMyc amplification is extremely rare in neuroblastoma, but a case study reports undifferentiated morphology, poor survival, and low levels of *MycN* expression in these tumors (62). These studies further support our hypothesis that physiological rather than overexpressed cMyc levels are associated with the better outcome of the disease.

Despite their very different endogenous roles during the development of the nervous system, it is important to keep in mind that all Myc family members have oncogenic properties and, upon misregulation, can trigger the onset of malignant transformation. In fact, in line with the reports on poor prognosis with very high cMyc levels, transcriptional profiles of downstream targets due to increased expression of any Myc member (MycN/cMyc/lMyc) are very similar in neuroblastoma and other cancer types, and all correlate with poor capacity to differentiate (63, 64). It is thus possible that some of the reports on forced MycN/cMyc overexpression in the sympathetic ganglia reflect this general oncogenic capacity instead of resembling the actual initiation process of neuroblastoma. Our results highlight the normal role of MycN in early neural development and raise the intriguing possibility that the balance of CIP2A/MycN binding at the neural plate border can influence cell-fate decisions in early embryos in a manner that triggers priming of neuroblastoma cells.

Materials and Methods

Detailed information regarding materials and methods can be found in *SI Appendix, SI Materials and Methods*. Briefly, whole-mount in situ hybridization and gain and loss of function experiments were performed on chicken embryos as previously described (65–67). Morpholinos were purchased from Gene Tools LLC (www.gene-tools.com/), immunostaining was performed as described (7), and Western blot lysates from the neuroblastoma cell lines SK-N-AS and SK-N-BE(2) were made 2 d after RNAi infection; the Western blot protocol was carried out as previously described (37, 68). Fluorescence on the images was quantified by using ImageJ (NIH). The PLA was performed according to the manufacturer's instructions for the Duolink kit (DUO92102; Sigma-Aldrich), and cell viability and proliferation was measured using the WST-1 kit (5015944001; Roche). The statistical analyses were performed on publicly available clinical neuroblastoma datasets (KOCAK, SEQC498, and Versteeg88) acquired from the R2 microarray analysis and visualization platform (https://hgserver1.amc.nl/cgi-bin/r2/main.cgi).

ACKNOWLEDGMENTS. We thank Dr. Marie Arsenian-Henriksson for providing SK-N-BE(2) cells, Dr. Kristina Cole for providing NGP cells, Dr. Ruth Palmer for providing SK-N-AS cells, and Dr. Edward K. Chan for the mouse monoclonal CIP2A antibody. This work was funded by NIH Grants HD037105 and DE024157 (to M.E.B.) and by grants from the Jane and Aatos Erkko Foundation, the Ella and Georg Ehrnrooth Foundation, and the Väre Foundation (to L.K.), the American-Scandinavian Foundation (to P.N.), and the Sigrid Juselius Foundation (to J.W.).

1. Matthay KK, et al. (2016) Neuroblastoma. *Nat Rev Dis Primers* 2:16078.
2. Maris JM (2010) Recent advances in neuroblastoma. *N Engl J Med* 362:2202–2211.
3. Brodeur GM, Seeger RC, Schwab M, Varmus HE, Bishop JM (1984) Amplification of N-myc in untreated human neuroblastomas correlates with advanced disease stage. *Science* 224:1121–1124.
4. Schwab M, et al. (1984) Chromosome localization in normal human cells and neuroblastomas of a gene related to c-myc. *Nature* 308:288–291.
5. Kerosuo L, Bronner-Fraser M (2012) What is bad in cancer is good in the embryo: Importance of EMT in neural crest development. *Semin Cell Dev Biol* 23:320–332.
6. Eilers M, Eisenman RN (2008) Myc's broad reach. *Genes Dev* 22:2755–2766.
7. Kerosuo L, Bronner ME (2016) cMyc regulates the size of the premigratory neural crest stem cell pool. *Cell Rep* 17:2648–2659.
8. Knoepfler PS, Cheng PF, Eisenman RN (2002) N-myc is essential during neurogenesis for the rapid expansion of progenitor cell populations and the inhibition of neuronal differentiation. *Genes Dev* 16:2699–2712.
9. Sawai S, et al. (1993) Defects of embryonic organogenesis resulting from targeted disruption of the N-myc gene in the mouse. *Development* 117:1445–1455.
10. Zinin N, et al. (2014) MYC proteins promote neuronal differentiation by controlling the mode of progenitor cell division. *EMBO Rep* 15:383–391.
11. Wakamatsu Y, Watanabe Y, Nakamura H, Kondoh H (1997) Regulation of the neural crest cell fate by N-myc: Promotion of ventral migration and neuronal differentiation. *Development* 124:1953–1962.
12. Charron J, et al. (1992) Embryonic lethality in mice homozygous for a targeted disruption of the N-myc gene. *Genes Dev* 6:2248–2257.
13. Khudyakov J, Bronner-Fraser M (2009) Comprehensive spatiotemporal analysis of early chick neural crest network genes. *Dev Dyn* 238:716–723.
14. Alam G, et al. (2009) MYCN promotes the expansion of Phox2B-positive neuronal progenitors to drive neuroblastoma development. *Am J Pathol* 175:856–866.
15. Pei D, et al. (2013) Distinct neuroblastoma-associated alterations of PHOX2B impair sympathetic neuronal differentiation in zebrafish models. *PLoS Genet* 9:e1003533.
16. Ke XX, et al. (2015) Phox2B correlates with MYCN and is a prognostic marker for neuroblastoma development. *Oncol Lett* 9:2507–2514.
17. Hirsch MR, Tiveron MC, Guillemot F, Brunet JF, Goridis C (1998) Control of noradrenergic differentiation and Phox2a expression by MASH1 in the central and peripheral nervous system. *Development* 125:599–608.
18. Vincentz JW, et al. (2012) A Phox2- and Hand2-dependent Hand1 cis-regulatory element reveals a unique gene dosage requirement for Hand2 during sympathetic neurogenesis. *J Neurosci* 32:2110–2120.
19. Pattyn A, Morin X, Cremer H, Goridis C, Brunet JF (1999) The homeobox gene Phox2b is essential for the development of autonomic neural crest derivatives. *Nature* 399: 366–370.
20. Sommer L, Shah N, Rao M, Anderson DJ (1995) The cellular function of MASH1 in autonomic neurogenesis. *Neuron* 15:1245–1258.
21. Wakamatsu Y, Watanabe Y, Shimono A, Kondoh H (1993) Transition of localization of the N-Myc protein from nucleus to cytoplasm in differentiating neurons. *Neuron* 10: 1–9.
22. Tsarovina K, et al. (2004) Essential role of Gata transcription factors in sympathetic neuron development. *Development* 131:4775–4786.
23. Nakagawara A, et al. (1993) Association between high levels of expression of the TRK gene and favorable outcome in human neuroblastoma. *N Engl J Med* 328:847–854.
24. Ernsberger U, Reissmann E, Mason I, Rohrer H (2000) The expression of dopamine beta-hydroxylase, tyrosine hydroxylase, and Phox2 transcription factors in sympathetic neurons: Evidence for common regulation during noradrenergic induction and diverging regulation later in development. *Mech Dev* 92:169–177.
25. Kramer M, Ribeiro D, Arsenian-Henriksson M, Deller T, Rohrer H (2016) Proliferation and survival of embryonic sympathetic neuroblasts by MYCN and activated ALK signaling. *J Neurosci* 36:10425–10439.
26. Sawai S, Kato K, Wakamatsu Y, Kondoh H (1990) Organization and expression of the chicken N-myc gene. *Mol Cell Biol* 10:2017–2026.
27. Edsjö A, et al. (2004) Neuroblastoma cells with overexpressed MYCN retain their capacity to undergo neuronal differentiation. *Lab Invest* 84:406–417.
28. Mobley BC, et al. (2015) Expression of MYCN in multipotent sympathoadrenal progenitors induces proliferation and neural differentiation, but is not sufficient for tumorigenesis. *PLoS One* 10:e0133897.
29. Olsen RR, et al. (2017) MYCN induces neuroblastoma in primary neural crest cells. *Oncogene* 36:5075–5082.
30. Li W, et al. (2008) CIP2A is overexpressed in gastric cancer and its depletion leads to impaired clonogenicity, senescence, or differentiation of tumor cells. *Clin Cancer Res* 14:3722–3728.
31. Chen KF, et al. (2010) CIP2A mediates effects of bortezomib on phospho-Akt and apoptosis in hepatocellular carcinoma cells. *Oncogene* 29:6257–6266.
32. Côme C, et al. (2009) CIP2A is associated with human breast cancer aggressivity. *Clin Cancer Res* 15:5092–5100.
33. Dong QZ, et al. (2011) CIP2A is overexpressed in non-small cell lung cancer and correlates with poor prognosis. *Ann Surg Oncol* 18:857–865.
34. Khanna A, et al. (2009) MYC-dependent regulation and prognostic role of CIP2A in gastric cancer. *J Natl Cancer Inst* 101:793–805.
35. Kerosuo L, et al. (2010) CIP2A increases self-renewal and is linked to Myc in neural progenitor cells. *Differentiation* 80:68–77.
36. Ventelä S, et al. (2012) CIP2A promotes proliferation of spermatogonial progenitor cells and spermatogenesis in mice. *PLoS One* 7:e33209.
37. Junttila MR, et al. (2007) CIP2A inhibits PP2A in human malignancies. *Cell* 130:51–62.
38. De Preter K, et al. (2006) Human fetal neuroblast and neuroblastoma transcriptome analysis confirms neuroblast origin and highlights neuroblastoma candidate genes. *Genome Biol* 7:R84, and erratum (2007) 8:401.
39. Rogers CD, Jayasena CS, Nie S, Bronner ME (2012) Neural crest specification: Tissues, signals, and transcription factors. *Wiley Interdiscip Rev Dev Biol* 1:52–68.
40. Roellig D, Tan-Cabugao J, Esaian S, Bronner ME (2017) Dynamic transcriptional signature and cell fate analysis reveals plasticity of individual neural plate border cells. *eLife* 6:e21620.
41. Cimadamore F, et al. (2011) Human ESC-derived neural crest model reveals a key role for SOX2 in sensory neurogenesis. *Cell Stem Cell* 8:538–551.
42. Khanna A, et al. (2013) Chk1 targeting reactivates PP2A tumor suppressor activity in cancer cells. *Cancer Res* 73:6757–6769.
43. Cohn SL, et al.; INRG Task Force (2009) The International Neuroblastoma Risk Group (INRG) classification system: An INRG Task Force report. *J Clin Oncol* 27:289–297.
44. Bellmeyer A, Krase J, Lindgren J, LaBonne C (2003) The protooncogene c-myc is an essential regulator of neural crest formation in xenopus. *Dev Cell* 4:827–839.
45. Hansford LM, et al. (2004) Mechanisms of embryonal tumor initiation: Distinct roles for MycN expression and MYCN amplification. *Proc Natl Acad Sci USA* 101: 12664–12669.
46. Chen X, Pappo A, Dyer MA (2015) Pediatric solid tumor genomics and developmental pliancy. *Oncogene* 34:5207–5215.
47. Narbonne-Reveau K, et al. (2016) Neural stem cell-encoded temporal patterning delineates an early window of malignant susceptibility in Drosophila. *eLife* 5:e13463.
48. Zhu S, Thomas Look A (2016) Neuroblastoma and its zebrafish model. *Adv Exp Med Biol* 916:451–478.
49. Corallo D, Candiani S, Ori M, Aveic S, Tonini GP (2016) The zebrafish as a model for studying neuroblastoma. *Cancer Cell Int* 16:82.
50. Weiss WA, Godfrey T, Francisco C, Bishop JM (2000) Genome-wide screen for allelic imbalance in a mouse model for neuroblastoma. *Cancer Res* 60:2483–2487.
51. Terrile M, et al. (2011) miRNA expression profiling of the murine TH-MYCN neuroblastoma model reveals similarities with human tumors and identifies novel candidate miRNAs. *PLoS One* 6:e28356.
52. Weiss WA, Aldape K, Mohapatra G, Feuerstein BG, Bishop JM (1997) Targeted expression of MYCN causes neuroblastoma in transgenic mice. *EMBO J* 16:2985–2995.
53. Williams P, Wegner E, Ziegler DS (2014) Outcomes in multifocal neuroblastoma as part of the neurocristopathy syndrome. *Pediatrics* 134:e611–e616.
54. Roshkow JE, Haller JO, Berdon WE, Sane SM (1988) Hirschsprung's disease, Ondine's curse, and neuroblastoma–Manifestations of neurocristopathy. *Pediatr Radiol* 19: 45–49.
55. Nemecek ER, Sawin RW, Park J (2003) Treatment of neuroblastoma in patients with neurocristopathy syndromes. *J Pediatr Hematol Oncol* 25:159–162.
56. Garavelli L, et al. (2015) Noonan syndrome-like disorder with loose anagen hair: A second case with neuroblastoma. *Am J Med Genet A* 167A:1902–1907.
57. Khanna A, Pimanda JE, Westermarck J (2013) Cancerous inhibitor of protein phosphatase 2A, an emerging human oncoprotein and a potential cancer therapy target. *Cancer Res* 73:6548–6553.
58. Dang CV (2012) MYC on the path to cancer. *Cell* 149:22–35.
59. Wang LL, et al. (2015) Augmented expression of MYC and/or MYCN protein defines highly aggressive MYC-driven neuroblastoma: A Children's Oncology Group study. *Br J Cancer* 113:57–63.
60. Wang LL, et al. (2013) Neuroblastoma of undifferentiated subtype, prognostic significance of prominent nucleolar formation, and MYC/MYCN protein expression: A report from the Children's Oncology Group. *Cancer* 119:3718–3726.
61. Zimmerman MW, et al. (2018) *MYC* drives a subset of high-risk pediatric neuroblastomas and is activated through mechanisms including enhancer hijacking and focal enhancer amplification. *Cancer Discov* 8:320–335.
62. Matsuno R, et al. (January 1, 2018) Rare MYC-amplified neuroblastoma with large cell histology. *Pediatr Dev Pathol*, 10.1177/1093526617749670.
63. Raetz EA, et al. (2003) Identification of genes that are regulated transcriptionally by Myc in childhood tumors. *Cancer* 98:841–853.
64. Fredlund E, Ringnér M, Maris JM, Påhlman S (2008) High Myc pathway activity and low stage of neuronal differentiation associate with poor outcome in neuroblastoma. *Proc Natl Acad Sci USA* 105:14094–14099.
65. Acloque H, Wilkinson DG, Nieto MA (2008) In situ hybridization analysis of chick embryos in whole-mount and tissue sections. *Methods Cell Biology* 87:169–185.
66. Kerosuo L, Bronner ME (2014) Biphasic influence of Miz1 on neural crest development by regulating cell survival and apical adhesion complex formation in the developing neural tube. *Mol Biol Cell* 25:347–355.
67. Sauka-Spengler T, Barembaum M (2008) Gain- and loss-of-function approaches in the chick embryo. *Methods Cell Biol* 87:237–256.
68. Kauko O, et al. (2015) Label-free quantitative phosphoproteomics with novel pairwise abundance normalization reveals synergistic RAS and CIP2A signaling. *Sci Rep* 5: 13099.